

## Article

# Effect of Vehicle Vibration on Interior Noise of Railway Vehicles Passing Through Rail Corrugation Sections

Junhyuk Lee <sup>1,2</sup> , Yonghyun Park <sup>1</sup> and Dahoon Ahn <sup>2,\*</sup> 

<sup>1</sup> Incheon Transit Corporation, 674, Gyeongin-ro, Namdong-gu, Incheon 21510, Republic of Korea; jh2msy@ictr.or.kr (J.L.); city4574@ictr.or.kr (Y.P.)

<sup>2</sup> Graduate School of Railway, Seoul National University of Science and Technology, 232 Gongneung-ro, Nowon-gu, Seoul 01811, Republic of Korea

\* Correspondence: dhahn@seoultech.ac.kr; Tel.: +82-2-970-6532

**Abstract:** This study involved experimental research to analyze the effect of rail corrugation on interior noise levels inside railway vehicles. Measurements taken on the Incheon Line 2 light rail indicated that the vehicle's age and maintenance condition have minimal effects on interior noise. Although wheel wear slightly reduces interior noise, it is insufficient to address the issue of abnormal noise. The analysis of the relationship between vehicle vibrations and interior noise revealed that at 80 km/h and with a 24 mm rail corrugation wavelength, vibrations at 920 Hz in the axle box and car body increase, coinciding with the dominant interior noise frequency of 926.6 Hz. Furthermore, an analysis using a car body sweep confirmed a relative increase in noise in the 920 Hz range. Therefore, abnormal noise in rail corrugation sections is caused by vibrations at 920 Hz due to the corrugation wavelength and train speed, which align with the car body resonance frequency, leading to increased car body vibrations and interior noise.

**Keywords:** noise; rail corrugation; vibration; natural frequency; resonance



**Citation:** Lee, J.; Park, Y.; Ahn, D. Effect of Vehicle Vibration on Interior Noise of Railway Vehicles Passing Through Rail Corrugation Sections. *Appl. Sci.* **2024**, *14*, 11447. <https://doi.org/10.3390/app142311447>

Academic Editor: Rosario Pecora

Received: 4 September 2024

Revised: 22 November 2024

Accepted: 27 November 2024

Published: 9 December 2024



**Copyright:** © 2024 by the authors. Licensee MDPI, Basel, Switzerland. This article is an open access article distributed under the terms and conditions of the Creative Commons Attribution (CC BY) license (<https://creativecommons.org/licenses/by/4.0/>).

## 1. Introduction

Urban railway vehicles serve as public transportation, carrying many people through urban areas. Noise can negatively affect both the surrounding environment and the safety and comfort of passengers. Recently, noise management has been implemented at the vehicle manufacturing stage to prevent railway noise issues, and operating organizations have established and implemented allowable standards of 80 dB for interior noise within vehicles. Vehicle noise includes rolling, aerodynamic, traction, structural, and pantograph noises, with varying contributions depending on the running speed. Rolling noise is generated by the contact between the wheels and rails. When the wheels run on the rails, excitation forces are generated by the irregular surface roughness of the wheels and rails, transmitting vibrations to the wheels, rails, and sleepers, which subsequently propagate as noise. Severe wear, irregular defects, and corrugation on the wheel and rail surfaces can worsen ride comfort and increase noise. Rail corrugation induces noise and vibration, which can damage vehicle components and degrade ride comfort. Consequently, various studies, including cause analyses, have been conducted to develop solutions for addressing corrugation issues.

Sato and Oostermeijer reviewed the literature on rail corrugation, detailing the formation mechanisms, effect analysis, prevention measures, and future research directions [1,2]. Wang systematically summarized the recent research results on the definition, classification, formation mechanisms, and detection methods of rail corrugation [3]. Grassie developed measurement equipment to understand rail corrugation characteristics and analyzed the formation and growth characteristics in different environments, studying the causes and preventive measures [4–6]. Meehan experimented with controlling the dynamic characteristics based on vehicle speed to predict and control the formation and growth of rail

corrugation [7]. Wang analyzed the causes of corrugation in sharp curves through field experiments and numerical analyses, studying the influence of rail inclination and vibration intensity on the formation of corrugation [8]. Zhang investigated the relationship between track structure dynamics and corrugation formation in curved sections and analyzed the correlation between vehicle speed and resonance phenomena [9]. Ling conducted experimental and numerical analyses on the effects of short-wavelength corrugation on slab-rail-fastening devices and proposed solutions [10]. Lei studied the effects of resonance phenomena caused by the overlap between the passing frequency in corrugation sections and the natural frequency of rail components on corrugation formation [11]. Balekwa analyzed short-wavelength rail corrugation sections through modal testing and finite element analysis to study the correlation between the axle and rail resonance phenomena [12]. Zhang presented methodologies for preventing short-wavelength corrugation based on a vehicle–rail model, finite element analysis, and validation [13].

Thompson developed a predictive model for rolling noise by measuring the surface roughness of wheels and rails and suggested noise reduction measures [14]. Eadie conducted long-term experiments with friction modifiers developed to reduce corrugation and noise in curved sections and documented the results [15]. Sadeghi compared the rolling noise of vehicles in straight and curved sections with rail corrugation by experimenting with the causes and characteristics of each section [16]. Han analyzed the effect of corrugation on interior noise by examining the noise, vibration, and roughness in slab rail corrugation sections [17]. Guo experimented with the effects of rail corrugation on interior noise by studying the quantitative relationship between wavelength and noise, and the noise reduction effect of rail grinding [18]. Peng investigated wheel–rail noise and interior noise due to rail corrugation and evaluated the noise effects of increased transverse stiffness and grinding of rails [19].

Previous studies have primarily focused on the formation mechanisms of corrugation, the effects on rail components and surrounding facilities, and the evaluation of noise levels of vehicles running through corrugation sections. Managing rail corrugation is important for enhancing the reliability and integrity of facilities; however, it is more crucial and essential to ensure the safe operation of vehicles and manage ride comfort issues such as noise and vibrations to prevent operational disruptions.

In this study, we conducted an experimental investigation to analyze the effects of rail corrugation on interior noise in railway vehicles. Typically, interior noise levels increase when railway vehicles pass through corrugated rail sections. However, as shown in this study, cases of abnormal noise level increases in specific frequency bands are rare. To identify the causes of this phenomenon, the research focused on the Incheon Line 2 light rail, where noise issues due to rail corrugation are severe. Interior noise levels were measured in corrugated rail sections under different vehicle maintenance conditions, and the correlation between vehicle vibration and interior noise was analyzed. Additionally, tests on vibration and noise characteristics were performed through excitation of the car body to comprehensively assess the impact of rail corrugation on interior noise.

## 2. Current Status of Rail Corrugation

### 2.1. Operating Line

Rail corrugations have been observed on Line 2 of the light rail transit operating in Incheon, South Korea. The total length of the line is 29.1 km one way, stretching from Unyeon Station to Geomdan-Oryu Station, and it comprises 27 stations. Recently, frequent occurrences of rail corrugations have been reported in several sections of this line, as shown in Figure 1. Table 1 presents the occurrence of rail corrugation on both the upper and lower lines. On the upper line, corrugation was found at 12 locations, covering 955 m, and on the lower line, it was found at 8 locations, covering 790 m. Although corrugation is generally known to occur more frequently in curved sections, the findings of this study revealed that most corrugations occurred in straight sections with higher vehicle speeds, except for two locations, which is a distinctive feature.

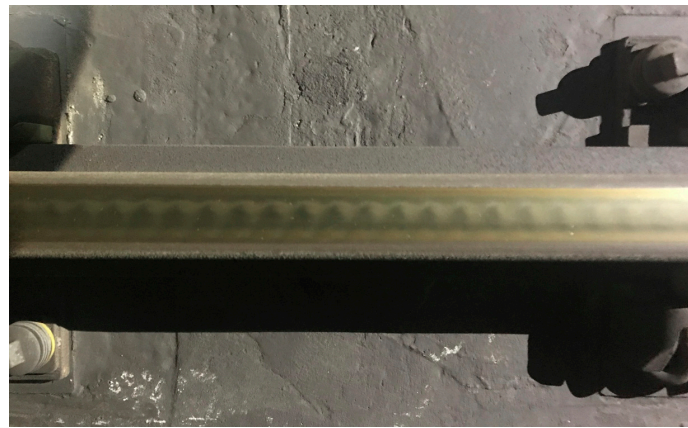


**Figure 1.** Rail corrugation.

**Table 1.** Status of rail corrugation.

Section	Direction	Location Start (m)	Location End (m)	Curve	Speed (km/h)
S2	down	1710	1790	-	72–78
	down	1850	1900	-	73–75
S4	up	3750	3870	-	79
S9	down	8520	8550	-	69
	down	8480	8540	-	69
	up	8480	8530	-	61–63
S10	down	9650	9750	-	53–67
	up	9230	9250	-	74
	up	9340	9400	-	79
	up	9420	9450	-	79
S11	up	10,250	10,370	-	74–79
	down	10,220	10,420	-	67–77
S12	down	11,570	11,640	-	57–59
	down	12,080	12,280	curve	34
	up	12,080	12,280	curve	25–30
S14	up	13,760	13,900	-	77–78
	up	13,920	13,985	-	63–74
S15	up	14,600	14,670	-	72–77
S24	up	25,070	25,110	-	59
S26	up	26,360	26,400	-	79

The light rail transit system consists of 43 trains, each comprising two cars, and operates autonomously. The maximum operational speed is 80 km/h, and the annual average mileage is approximately 120,000 km, which is substantial. The power supply method for the LRT is a third rail system, and the wheels are equipped with resilient wheels that exhibit excellent noise and vibration damping performance. Figure 2 shows the Incheon Line 2 LRT vehicle, and Table 2 presents the specifications of the LRT vehicle.

**Table 2.** Specifications of LRT vehicle.

Item	Specification
Composition	1 unit (2 cars): MC1–MC2
Weight	1 unit: 63.0 tons, Empty: 31.5 tons/car, Max.: 44.3 tons/car

Table 2. Cont.

Item	Specification
Dimensions	Length: 34.4 m, Width: 2.65 m, Height: 3.4 m
Passengers	206 (Seated 58, Standing 148)
Max. Speed	80 km/h
Bogie	Bolsterless Bogie
Wheel	Resilient Wheel
Power Supply System	Third Rail



Figure 2. LRT vehicle.

### 2.2. Interior Noise Levels

Recently, numerous occurrences of rail corrugation have been discovered in various operational sections, and as a result, the level of abnormal interior noise has also increased. Figure 3 shows the equivalent noise levels and maximum values measured in the light rail vehicle during commercial operation, segmented by sections between stations. The equivalent noise level for each section was calculated by averaging the interior noise from departure to arrival at each station, and the maximum value represents the highest noise level measured in each section. The average equivalent noise level was 81.8 dB, and the maximum value was 89.5 dB. The average maximum noise level was 91.3 dB, with the highest value recorded at 101.6 dB, which is significantly high. These results significantly exceed the interior noise standard of 80 dB managed by the urban railway operating organization, deteriorating passenger comfort during commercial operations and leading to an increase in noise complaints. Further research is required to identify the causes of these abnormal noise occurrences.

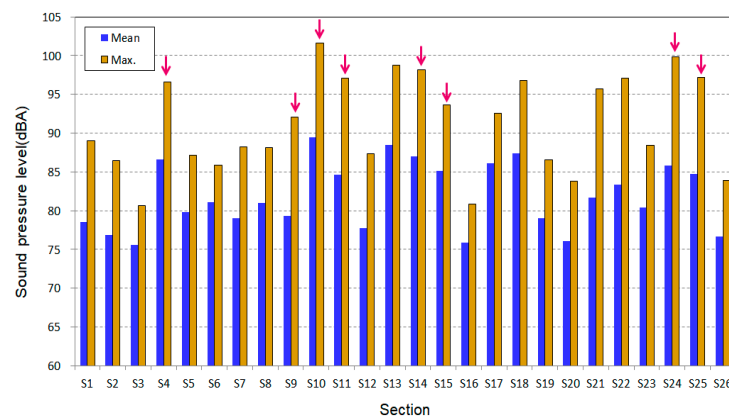
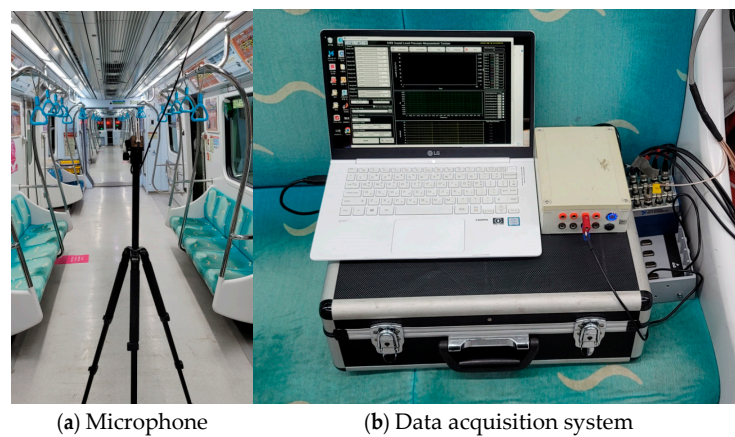


Figure 3. Interior noise levels of LRT vehicles (↓: sections with rail corrugation).

### 3. Noise Characteristics According to Vehicle Maintenance Conditions

This study aims to identify the effect of vehicle maintenance conditions on abnormal interior noise by performing interior noise measurements under different maintenance conditions. International standards for noise measurement include ISO 3381, GB/T 3449-2011, and JIS E 4021-2008. In this study, noise measurements were conducted in accordance with KS I ISO 3381, which is identical to the widely adopted ISO 3381 [20–23]. As shown in Figure 4a, noise sensors were installed inside the vehicle, and the noise recorded during operation was stored using the data storage device shown in Figure 4b. Four test vehicles were selected, each reflecting different maintenance conditions, as shown in Table 3. Interior noise levels were measured during operation for each case, and equivalent noise levels were analyzed for segments between stations.



**Figure 4.** Interior noise measurement equipment.

**Table 3.** Test conditions according to vehicle maintenance status.

Case	Year of Vehicle Manufacture	Wheel Diameter (mm)	Wheel Profile State	Remark
1	2012	621	worn	before heavy maintenance
2	2012	660	new	after heavy maintenance
3	2012	618	new	after wheel reprofiling
4	2022	660	moderate	new vehicle

- (1) Case 1: Vehicle just before a major overhaul, conducted every 4 years, with a wheel diameter reduced to 621 mm from the original 660 mm and with worn wheel treads.
- (2) Case 2: The same vehicle as in Case 1, but after a major overhaul, with new wheels installed, a wheel diameter of 660 mm, and freshly machined wheel treads.
- (3) Case 3: Vehicle with wheels machined due to damage during operation, with a wheel diameter of 618 mm and machined wheel treads in their original condition.
- (4) Case 4: Recently manufactured vehicle with a wheel diameter of 660 mm and moderately worn wheel treads after accumulating approximately 50,000 km of service.

Figure 5 and Table 4 present the equivalent interior noise levels measured in each section under all vehicle maintenance conditions. Overall, the noise levels in sections with rail corrugation were significantly high, showing a similar trend across the different maintenance conditions of the vehicles.

In Case 1, which had the poorest maintenance condition, the average noise level across all sections was 80.6 dB, with a maximum value of 89.2 dB. In contrast, the vehicle in Case 2, which completed a major overhaul, exhibited an average noise level of 79.9 dB and a maximum of 85.9 dB. The vehicle in Case 3, with only machined wheels, recorded an average noise level of 79.6 dB and a maximum of 86.0 dB. Compared to Case 1, Cases

2 and 3 showed a slight reduction of approximately 1.0 dB in the average noise levels; however, the maximum values decreased by more than 3 dB. These findings indicate that wheel machining contributes to a reduction in interior noise. Comparing Cases 2 and 3, the noise levels were nearly identical, suggesting that other inspection items during the major overhaul, aside from the wheel machining, had little effect on the interior noise during operation.

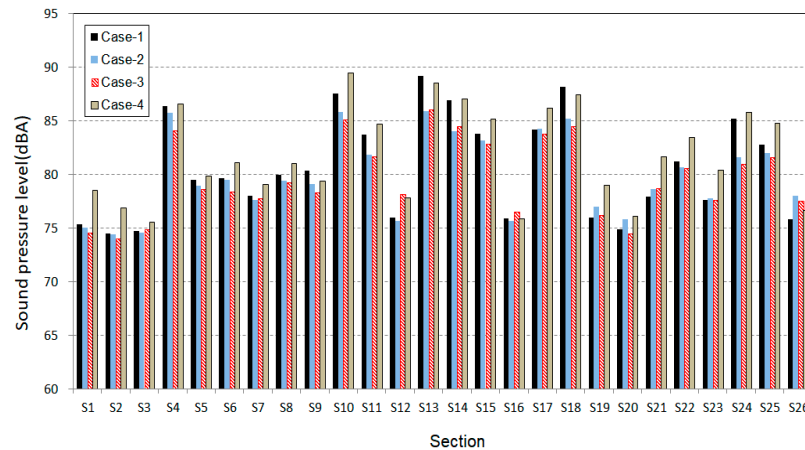


**Figure 5.** Interior noise levels according to vehicle maintenance status.

**Table 4.** Results of interior noise measurements according to vehicle maintenance status (dBA).

Item	Case 1	Case 2	Case 3	Case 4
Mean	80.6	79.9	79.6	81.8
Maximum	89.2	85.9	86.0	89.5

In summary, suspension system components affecting the vehicle's dynamic performance are managed within specific material property limits according to maintenance regulations, resulting in minimal differences in material properties before and after maintenance. Other inspection tasks are limited to exterior inspections, vehicle cleaning, and consumable replacements, with maintenance related to interior noise primarily involving cleaning.

Additionally, both the wheels of Case 2 and Case 3 were re-profiled according to design specifications, and despite differences in wheel diameters, the difference in interior noise was minimal. This suggests that wheel diameter has a negligible effect on interior noise. Case 4 showed the highest noise levels, with an average of 81.8 dB and a maximum of 89.5 dB among the four test conditions. Although this vehicle is relatively new and in good condition, the high noise levels are likely due to differences in body noise characteristics resulting from variations in manufacturing practices of the current manufacturer compared to previous ones.

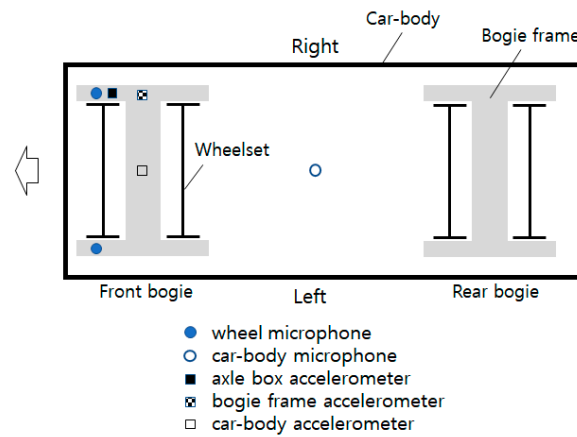
Therefore, vehicle maintenance conditions, particularly wheel re-profiling, have a measurable effect on interior noise. However, in sections with rail corrugation, the influence of maintenance conditions on interior noise is not significant enough to provide a fundamental solution to abnormal noise issues.

#### 4. Identification of the Causes of Abnormal Noise

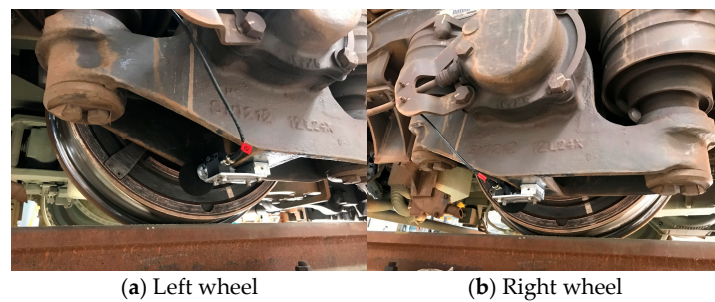
To identify the causes of abnormal noise due to rail corrugation and analyze the noise transmission path, noise measurements were taken not only inside the vehicle, but also on the wheels during operation.

Figure 6 shows the positions of the vibration and noise sensors, while Figure 7 shows the noise sensors installed on the left and right wheels of the first axle in the direction of running. Additionally, to analyze the noise transmission path, vibrations were measured at

key parts of the vehicle, including the axle box, bogie, and car body. As shown in Figure 8, accelerometers were installed on the right axle box and the upper side frame of the right bogie to measure the wheelset vibrations. Furthermore, accelerometers were installed on the floor of the car body above the front bogie to measure the car body vibrations. Table 5 presents the specifications and installation locations of the sensors.



**Figure 6.** Sensor (microphone, accelerometer) installed locations.



**Figure 7.** Microphones installed on the vehicle.

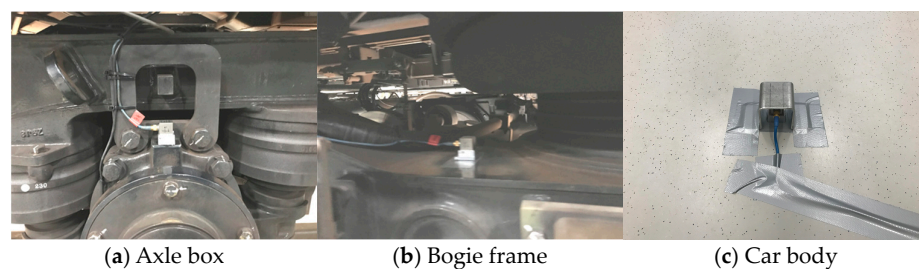


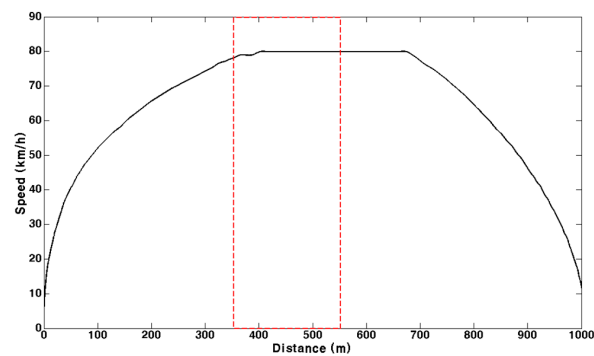
**Figure 8.** Accelerometers installed on the vehicle.

The test section was selected as the S10 upline section, where the highest noise levels were observed among the corrugated sections, as shown in Figure 3. Corrugation was observed in the 350–550 m section, and the vehicle speed was maintained at the same level as the commercial operation speed. Figure 9 presents the vehicle speed, axle box, bogie frame, car body accelerations, and wheel and car body noise data measured in the S10 section.

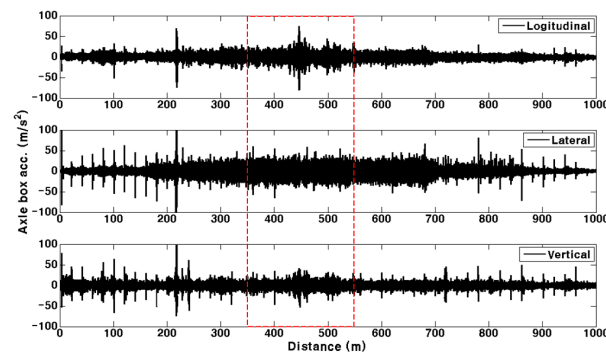
Figure 10 shows the results of calculating the RMS of the measured accelerations and noise data every 10 m and converting them into dB units. The noise signal was an A-weighted sound level adjusted for auditory perception. It was confirmed that the wheel and interior noises significantly increased when passing through the 350–550 m rail corrugation section. The interior noise levels reached 102.7 dB in the rail corrugation section, and the accelerations increased in the vertical direction of the axle box and the longitudinal, lateral, and vertical directions of the car body.

Table 5. Accelerometer and microphone specifications.

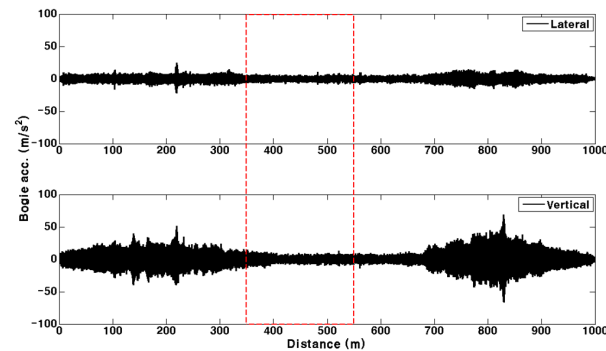
Item		Measurement Location	Measurement Direction	Sensor Specification
Accelerometer	Wheel	Longitudinal front axle right side journal box	Longitudinal Lateral Vertical	Kistler triaxial accelerometer, $\pm 50$ g
	Bogie	Longitudinal front bogie right side frame top	Lateral Vertical	
	Car body	Longitudinal front bogie center body bottom	Longitudinal Lateral Vertical	
Microphone	Right wheel	Longitudinal front axle right side journal box	-	PCB 1/2 prepolarized free-field condenser microphone, 50 mV/Pa, 3.75–20 kHz
	Left wheel	Longitudinal front axle left side journal box	-	
	Car body	Center of the car body, height 1.6 m	-	



(a) Vehicle speed

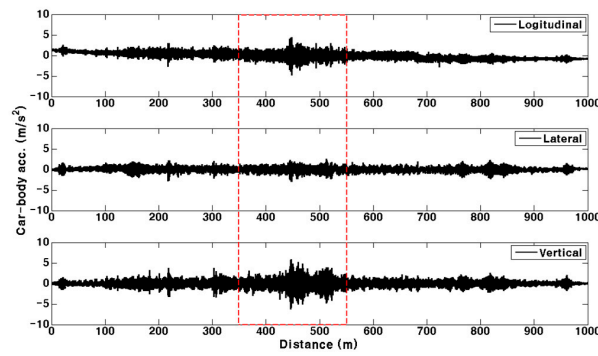


(b) Axle box acceleration

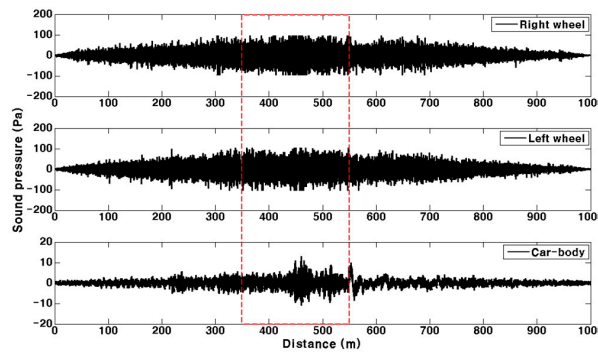


(c) Bogie acceleration

Figure 9. Cont.



(d) Car body acceleration



(e) Wheel and car body noise

Figure 9. Acceleration and noise data measured in the rail corrugation section (□).

To analyze the relationship between vibration and noise in the rail corrugation section, the correlation between the vibration acceleration of various vehicle components and interior noise was examined at the maximum noise point (located at 425–525 m). The results of the correlation analysis between the RMS of axle box, bogie, and car body vibrations, measured every 10 m, and interior noise are shown in Table 6 and Figure 11. Vibrations with relatively high correlations included the vertical vibration of the axle box and the longitudinal, lateral, and vertical vibrations of the car body. Among these, the vertical vibration of the car body showed the highest correlation with interior noise, at 0.95. These results indicate that interior noise is strongly influenced by car body vibrations.

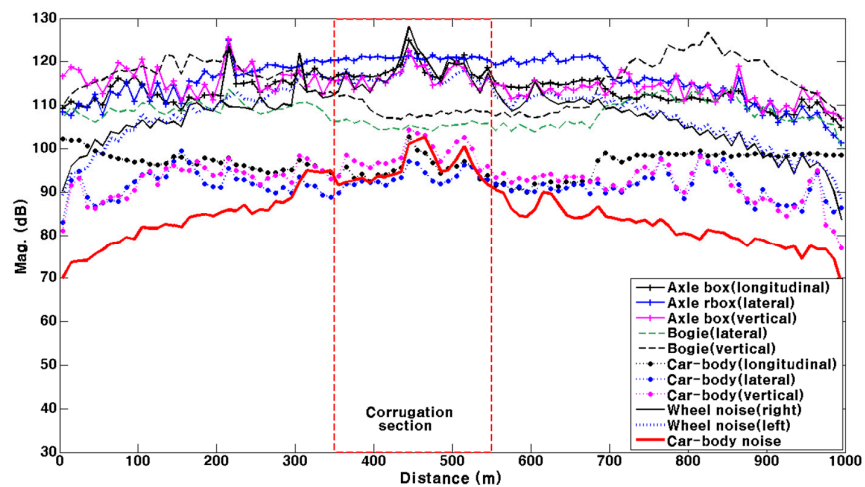


Figure 10. Acceleration and noise data analyzed at 10 m intervals.

Table 6. Correlation between vehicle vibration and interior noise.

Correlation	Axle Box Longitudinal (1)	Axle Box Lateral (2)	Axle Box Vertical (3)	Bogie Lateral (4)	Bogie Vertical (5)	Car Body Longitudinal (6)	Car Body Lateral (7)	Car Body Vertical (8)
Noise	0.44	0.06	0.59	0.19	0.20	0.84	0.82	0.95

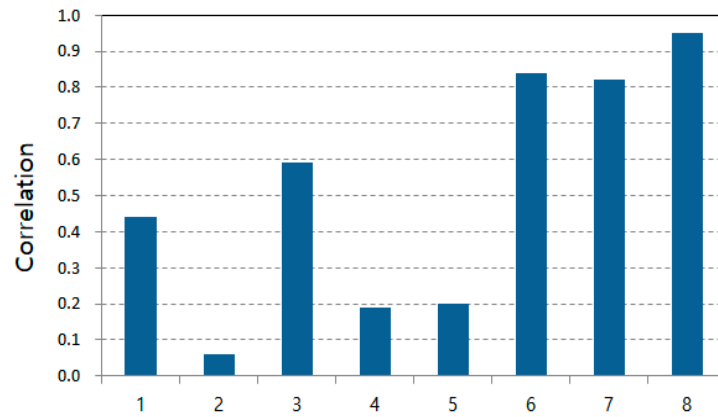


Figure 11. Correlation between vehicle vibration and interior noise in the maximum noise section.

For a more detailed analysis, the frequency characteristics of the noise and vibrations were analyzed based on the presence of corrugation while the vehicle was operating at 80 km/h. Figure 12 shows the frequency analysis results for interior noise. Compared to sections without corrugation, the frequency characteristics in the corrugated section increased significantly in the 920 Hz band, and its multiples, 1840 Hz, 2760 Hz, and 3680 Hz, also increased. Figure 13 shows the frequency analysis results of the vertical vibrations of the axle box and car body, which exhibited a high correlation with the interior noise. Similar to the interior noise frequency analysis, it was confirmed that the vertical vibrations of the axle box and car body increased significantly in the 920 Hz band when passing through the rail corrugation section. This aligns with the previous correlation analysis results, confirming that the vertical vibrations of the axle box and car body strongly correlate with interior noise.

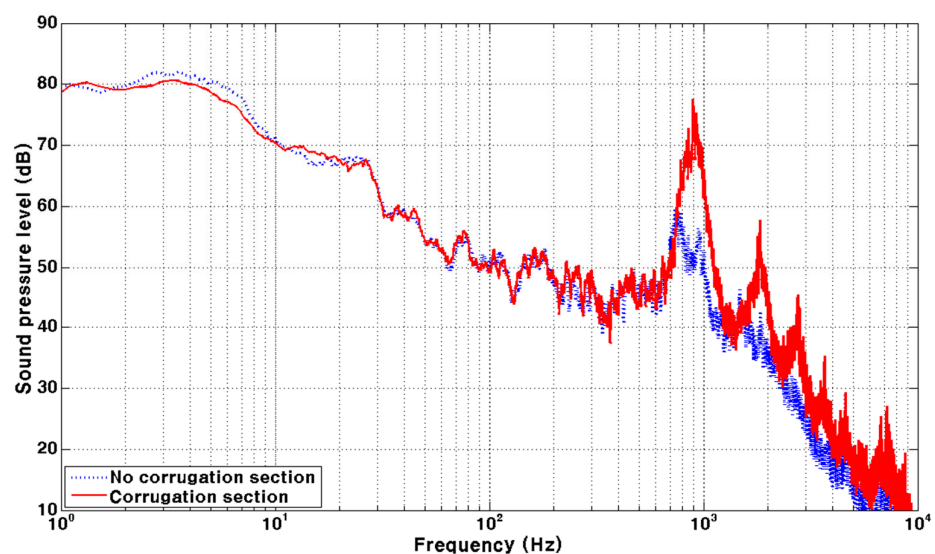
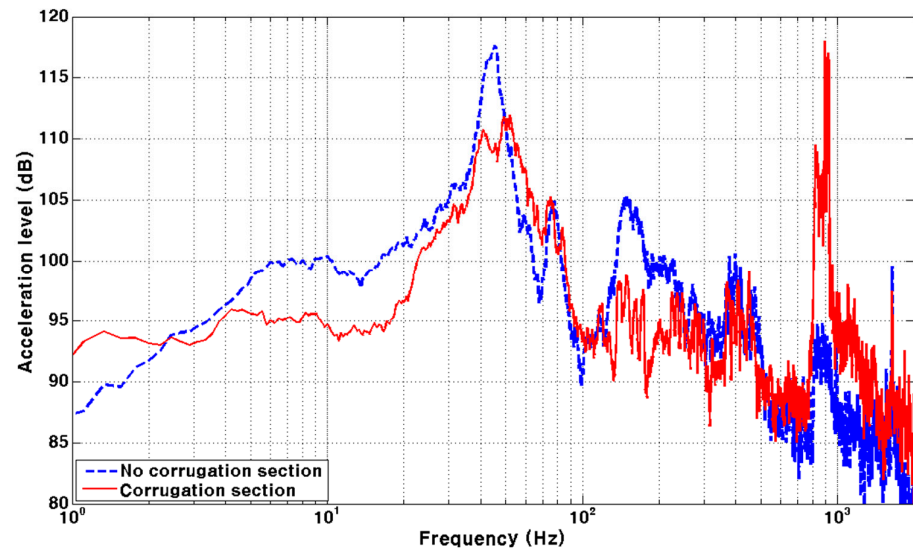


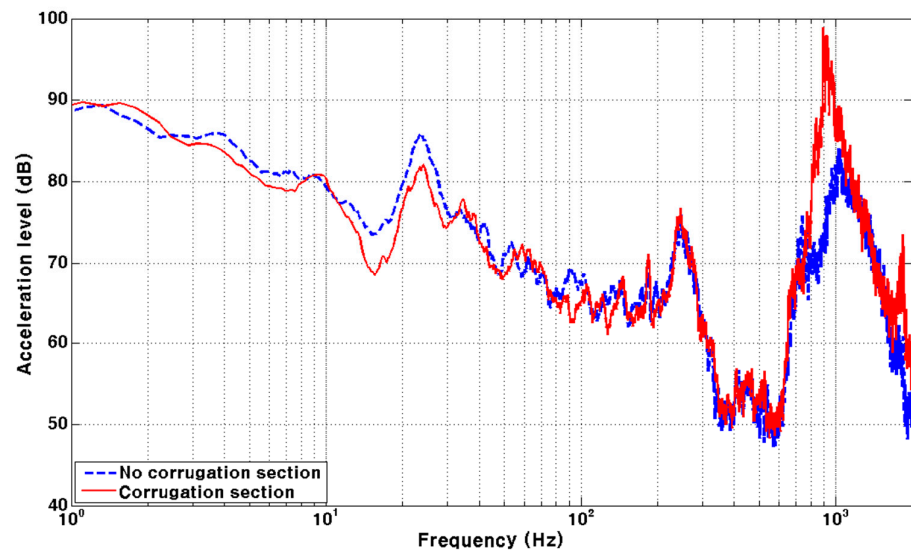
Figure 12. Interior noise in section with or without corrugation.

Considering the vibration transmission path during vehicle operation, it can be inferred that when passing through the rail corrugation section, the 920 Hz band vibration is

excited in the vertical direction of the wheelset, which is then transmitted to the vertical vibration of the car body, influencing the interior noise frequency.



(a) Axle box vertical acceleration



(b) Car body vertical acceleration

**Figure 13.** Axle box and car body acceleration in section with or without corrugation.

To analyze the increase in the 920 Hz band vibration frequency, the S10 section, where corrugation occurred, was examined. Figure 14 shows the rail corrugation in the S10 section. The wavelength of the corrugation was 24 mm, and when the vehicle was operated at 80 km/h, the vibration frequency caused by the corrugation, calculated using Equation (1), was 926 Hz. Here,  $V$  is the vehicle speed, and  $\lambda$  is the wavelength of the corrugation.

$$f(\text{Hz}) = (V \times 1000) / 3.6\lambda \tag{1}$$

Based on this result, it can be confirmed that the 920 Hz frequency, which dominates the interior noise when passing through the rail corrugation section, matches the excitation vibration frequency of 926 Hz generated when passing through the rail corrugation section. Considering the vibration transmission path in the vehicle, the 926 Hz vibration induced by passing through the rail corrugation section is transmitted to the vertical vibration of

the axle box, which subsequently excites the car body, matching the car body's resonance mode and resulting in increased interior noise. A test was conducted to verify the interior noise characteristics caused by the car body vibrations.



**Figure 14.** Rail corrugation in the S10 section.

Figure 15 shows the setup used for testing the vibration and noise characteristics of the car body. An exciter was installed on the underframe of the car body, and the exciter and frame were connected using a stinger. An impedance head was installed at the end of the stinger on the underframe side to measure the input excitation force and response, and a frequency analyzer was used to test the natural frequency of the car body. Accelerometers and noise sensors were installed inside the vehicle to analyze the effect of car body excitation on interior noise. Table 7 lists the specifications of the car body noise characteristic test device.

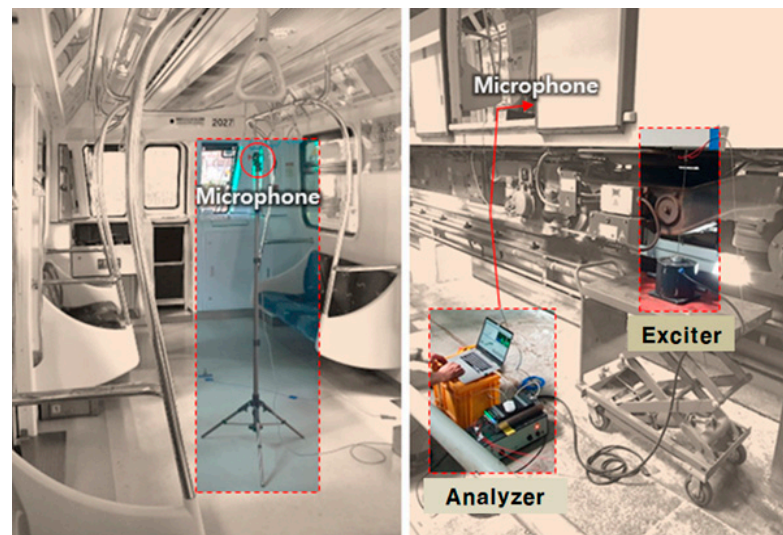


**Figure 15.** The equipment for car body noise characteristics.

Figure 16 shows the results of testing the natural frequency of the car body according to the under-body excitation. Frequencies related to the 920 Hz abnormal noise frequency observed during the rail corrugation section operation, such as 884.4 Hz and 926.6 Hz, were detected. These frequency bands have very low damping ratios, indicating a high possibility of car body resonance. To confirm this, the interior noise was measured by sweeping the frequency band at approximately 900 Hz, which is the car body resonance frequency. Figure 17 shows the results of the car body noise characteristic test, confirming that the noise around (yellow section) the car body resonance frequency of 920 Hz increased.

Therefore, it is concluded that the abnormal noise observed during rail corrugation section operation is caused by 920 Hz vibrations induced when the vehicle operates at 80 km/h through a rail corrugation section with a wavelength of 24 mm, transmitted vertically through the axle box and car body. The 920 Hz band vibration of the car body matches the car body's resonance frequency of 926.6 Hz, resulting in increased interior noise.

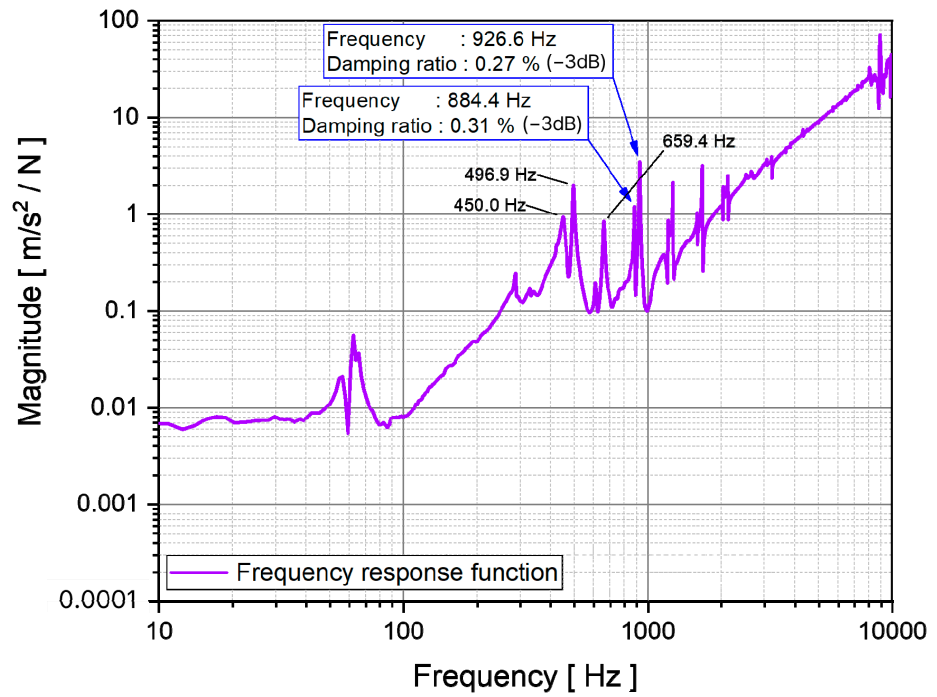


Figure 16. Car body vibration characteristics.

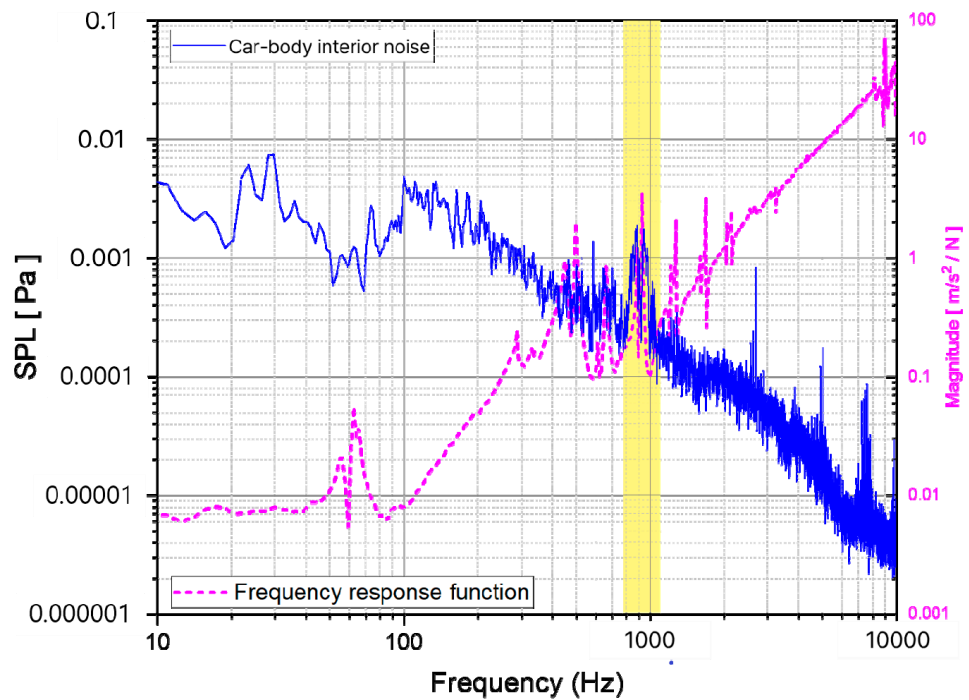


Figure 17. Interior noise characteristics.

**Table 7.** Specifications of the equipment for car body noise characteristics.

Equipment	Specification
FFT analyzer	Bruel & Kjaer Lan-xi 3160-A-042 Brüel & Kjær, Nærum, Denmark
Exciter	Bruel & Kjaer 4808 (frequency range: 5–10 kHz) Brüel & Kjær, Nærum, Denmark
Impedance head	Dytran 58608 Dytran Instruments, Inc. Chatsworth, California, USA.
Microphone	PCB 378B02 (frequency range: 3.75–20 kHz) PCB Piezotronics, Inc., Depew, New York, USA.
Conditioning amplifier	Bruel & Kjaer 2690 Brüel & Kjær, Nærum, Denmark
Accelerometer	PCB 393B04 PCB Piezotronics, Inc., Depew, New York, USA.

## 5. Conclusions

The causes of abnormal noise in light rail vehicles passing through sections with rail corrugation were identified, and the following observations were made:

- (1) The measurement of interior noise in rail corrugation sections under different vehicle maintenance conditions indicated that the influence of the vehicle's age or maintenance conditions is minimal. Although the wear state of the wheels slightly reduces the interior noise, it is insufficient to solve the problem of abnormal noise.
- (2) An investigation of the rail corrugation section revealed that the corrugation wavelength was 24 mm, and vibrations in the 920 Hz range were induced when the vehicle operated at a maximum speed of 80 km/h.
- (3) The vertical vibrations of the axle box and car body strongly correlated with the abnormal interior noise frequency of 926 Hz.
- (4) The natural frequency test of the car body through excitation identified natural frequencies of 884.4 Hz and 926.6 Hz. The analysis of the interior noise effect through car body sweep excitation confirmed a relative increase in noise in the 920 Hz range, which corresponds to the car body's resonance frequency.

Therefore, the abnormal noise that occurs when the vehicle passes through the rail corrugation section is induced by 920 Hz vibrations caused by the wavelength of the corrugation and the vehicle speed. These vibrations are transmitted to the car body, matching the car body's resonance frequency of 926.6 Hz, resulting in increased interior noise.

Based on these results, reducing abnormal noise when passing through corrugated sections may require avoiding the 920 Hz resonance mode of the car body. However, this would require either replacing the car body or performing extensive maintenance to improve car body noise characteristics, which is challenging in practice. As an alternative, future studies will explore standard rail grinding methods or adjustments to vehicle speed and braking control when passing through corrugated sections to mitigate corrugation formation.

Additionally, although corrugation typically occurs on curved sections, it was mainly observed on straight sections in this study. Further research is also needed to investigate whether the shorter wavelength of corrugation is related to the use of resilient wheels.

**Author Contributions:** Conceptualization, J.L. and D.A.; methodology, J.L.; software, J.L. and Y.P.; validation and formal analysis, D.A.; investigation, Y.P.; resources and data curation, Y.P.; writing—original draft preparation, J.L. and Y.P.; writing—review and editing, J.L. and D.A.; visualization, Y.P.; supervision, J.L. and D.A.; project administration, J.L.; funding acquisition, Y.P. All authors have read and agreed to the published version of the manuscript.

**Funding:** This research was supported by the National Research and Development Program (RS-2021-KA163504) funded by the Ministry of Land, Infrastructure and Transport.

**Institutional Review Board Statement:** Not applicable.

**Informed Consent Statement:** Not applicable.

**Data Availability Statement:** Data are contained within the article.

**Conflicts of Interest:** Authors Junhyuk Lee and Yonghyun Park were employed by Incheon Transit Corporation. The remaining author declare that the research was conducted in the absence of any commercial or financial relationships that could be construed as a potential conflict of interest.

## References

1. Sato, Y.; Matsumoto, A.; Knothe, K. Review on rail corrugation studies. *Wear* **2002**, *253*, 130–139. [[CrossRef](#)]
2. Oostermeijer, K.H. Review on short pitch rail corrugation studies. *Wear* **2008**, *265*, 1231–1237. [[CrossRef](#)]
3. Wang, Q.A.; Huang, X.Y.; Wang, J.F.; Ni, Y.Q.; Ran, S.C.; Li, J.P.; Zhang, J. Concise Historic Overview of Rail Corrugation Studies: From Formation Mechanisms to Detection Methods. *Buildings* **2024**, *14*, 968. [[CrossRef](#)]
4. Grassie, S.L. Short wavelength rail corrugation: Field trials and measuring technology. *Wear* **1996**, *191*, 149–160. [[CrossRef](#)]
5. Grassie, S.L. Rail corrugation: Advances in measurement, understanding and treatment. *Wear* **2005**, *258*, 1224–1234. [[CrossRef](#)]
6. Grassie, S.L. Rail corrugation: Characteristics, causes, and treatments. *Proc. Inst. Mech. Eng. Part F J. Rail Rapid Transit* **2009**, *223*, 581–596. [[CrossRef](#)]
7. Meehan, P.A.; Bellette, P.A.; Batten, R.D.; Daniel, W.J.T.; Horwood, R.J. A case study of wear-type rail corrugation prediction and control using speed variation. *J. Sound Vib.* **2009**, *325*, 85–105. [[CrossRef](#)]
8. Wang, Z.; Lei, Z.; Zhu, J. Study on the formation mechanism of rail corrugation in small radius curves of metro. *J. Mech. Sci. Technol.* **2023**, *37*, 4521–4532. [[CrossRef](#)]
9. Zhang, H.G.; Liu, W.N.; Liu, W.F.; Wu, Z.Z. Study on the cause and treatment of rail corrugation for Beijing metro. *Wear* **2014**, *317*, 120–128. [[CrossRef](#)]
10. Ling, L.; Li, W.; Shang, H.; Xiao, X.; Wen, Z.; Jin, X. Experimental and numerical investigation of the effect of rail corrugation on the behaviour of rail fastenings. *Veh. Syst. Dyn.* **2014**, *52*, 1211–1231. [[CrossRef](#)]
11. Lei, Z.; Wang, Z. Generation Mechanism and Development Characteristics of Rail Corrugation of Cologne Egg Fastener Track in Metro. *KSCE J. Civ. Eng.* **2020**, *24*, 1763–1774. [[CrossRef](#)]
12. Balekwa, B.M.; Kallon, D.V.V. Correlation of Short Pitch Rail Corrugation with Railway Wheel-Track Resonance at Low Frequencies of Excitation. *Vibration* **2020**, *3*, 491–520. [[CrossRef](#)]
13. Zhang, P.; Li, S.; Li, Z. Short pitch corrugation mitigation by rail constraint design. *Int. J. Mech. Sci.* **2023**, *243*, 108037. [[CrossRef](#)]
14. Thompson, D.J. On the Relationship Between Wheel and Rail Surface Roughness and Rolling Noise. *J. Sound Vib.* **1996**, *193*, 149–160. [[CrossRef](#)]
15. Eadie, D.T.; Santoro, M. Top-of-rail friction control for curve noise mitigation and corrugation rate reduction. *J. Sound Vib.* **2006**, *293*, 747–757. [[CrossRef](#)]
16. Sadeghi, J.; Hasheminezhad, A. Correlation between rolling noise generation and rail roughness of tangent tracks and curves in time and frequency domains. *Appl. Acoust.* **2016**, *107*, 10–18. [[CrossRef](#)]
17. Han, J.; Xiao, X.B.; Wu, Y.; Wen, Z.F.; Zhao, G.T. Effect of rail corrugation on metro interior noise and its control. *Appl. Acoust.* **2018**, *130*, 63–70. [[CrossRef](#)]
18. Guo, J.Q.; Zhu, L.W.; Liu, X.L.; Han, J.; Xiao, X.B. Experimental and Simulation Study on the Relationship between Interior Noise of Metro Cab and Rail Corrugation. *J. Mech. Eng.* **2019**, *55*, 141–147.
19. Peng, H.; Yao, Y.; Cai, X.; Zhong, Y.; Sun, T. Field Measurement Analysis and Control Measures Evaluation of Metro Vehicle Noise Caused by Rail Corrugation. *Appl. Sci.* **2021**, *11*, 11190. [[CrossRef](#)]
20. *ISO 3381:2021(E)*; Railway Applications–Acoustics–Noise Measurement Inside Railbound Vehicles. International Organization for Standardization: Geneva, Switzerland, 2021.
21. *GB/T 3449-2011*; Acoustics—Measurement of Noise Inside Railbound Vehicles. Standardization Administration of China (SAC): Beijing, China, 2011.
22. *JIS E 4021:2008*; Acoustics—Measurement of Noise Inside Railbound Vehicles. Japanese Industrial Standards Committee (JISC): Tokyo, Japan, 2008.
23. *KS I ISO 3381:2020*; Railway Application–Acoustics–Measurement of Noise Inside Railbound Vehicles. Korea Industrial Standards (KAST): Seoul, Republic of Korea, 2020.

**Disclaimer/Publisher’s Note:** The statements, opinions and data contained in all publications are solely those of the individual author(s) and contributor(s) and not of MDPI and/or the editor(s). MDPI and/or the editor(s) disclaim responsibility for any injury to people or property resulting from any ideas, methods, instructions or products referred to in the content.